

What have we learned from intensive atmospheric sampling field programmes of CO₂?

By J. C. LIN^{1*}, C. GERBIG², S. C. WOFYSY³, B. C. DAUBE³, D. M. MATROSS³, V. Y. CHOW³, E. GOTTLIEB³, A. E. ANDREWS⁴, M. PATHMATHEVAN³ and J. W. MUNGER³

¹Department of Atmospheric Science, Colorado State University, 1371 Campus Delivery, Fort Collins, CO 80523-1371, USA; ²Max-Planck-Institut für Biogeochemie, Hans-Knoell-Str. 10, D-07745 Jena, Germany;

³Department of Earth & Planetary Science and, Division of Engineering & Applied Sciences, Harvard University, 20 Oxford St., Cambridge, MA 02138, USA; ⁴Climate Monitoring and Diagnostics Laboratory, National Oceanographic and Atmospheric Administration, 325 Broadway, Boulder, CO 80305-3328, USA

(Manuscript received 24 November 2005; in final form 2 June 2006)

ABSTRACT

The spatial and temporal gradients in atmospheric CO₂ contain signatures of carbon fluxes, and as part of inverse studies, these signatures have been combined with atmospheric models to infer carbon sources and sinks. However, such studies have yet to yield finer-scale, regional fluxes over the continent that can be linked to ecosystem processes and ground-based observations. The reasons for this gap are twofold: lack of atmospheric observations over the continent and model deficiencies in interpreting such observations.

This paper describes a series of intensive atmospheric sampling field programmes designed as pilot experiments to bridge the observational gap over the continent and to help test and develop models to interpret these observations. We summarize recent results emerging from this work, outlining the role of the intensive atmospheric programmes in collecting CO₂ data in both the vertical and horizontal dimensions. These data: (1) quantitatively establish the spatial variability of CO₂ and the associated errors from neglecting this variability in models; (2) directly measure regional carbon fluxes from air-mass-following experiments and (3) challenge models to reduce and account for uncertainties in atmospheric transport. We conclude with a look towards the future, outlining ways in which intensive atmospheric sampling can contribute towards advancing carbon science.

1. Introduction

Atmospheric observations of CO₂ have contributed greatly to current understanding of the modern carbon cycle. The multi-decadal time series of CO₂ concentrations at Mauna Loa provided conclusive evidence of long-term build-up of CO₂ from human activities and seasonal variations from biospheric fluxes (Keeling et al., 1976). More recently, the observed distributions of CO₂ have been combined with models of atmospheric transport as part of ‘inverse studies’—which solve for carbon fluxes that are consistent with the CO₂ distributions—to suggest the presence of a large terrestrial carbon sink in the northern mid-latitudes (Tans et al. 1990).

The pioneering study by Tans et al. (1990), was followed up by numerous other inverse studies which corroborated the existence

of a northern mid-latitude terrestrial carbon sink (Enting et al., 1995; Fan et al., 1998; Bousquet et al., 1999; Gurney et al., 2002). However, due to model limitations and paucity of continental CO₂ observations (see below) these studies have disagreed about the partitioning of the northern sink between Eurasia (Bousquet et al., 1999) versus North America (Fan et al., 1998) and have yielded carbon fluxes only at coarse resolution, over large spatial regions. For example, one recent inverse study (Gurney et al., 2002) retrieved carbon fluxes over 22 areas around the Earth, with lengthscale of each area reaching 1000–10000 km.

Atmospheric inverse methods have to provide flux information at a much finer scale (10–1000 km) than current estimates in order to compare with information about terrestrial processes on the ecosystem scale. One of the goals of carbon cycle science is to use the valuable information that atmospheric measurements can provide to inform and test against knowledge about terrestrial processes from ground-based measurements (Wofsy et al., 1993; Barford et al., 2001) and models (Schimel et al., 2000). Reconciling observed carbon fluxes with casual mechanisms across scales is a key focus of carbon cycle science in recent

*Corresponding author address: Department of Earth Sciences, University of Waterloo, 200 University Ave. W., Waterloo, ON, Canada N2L 3G1.

e-mail: jcl@uwaterloo.ca

DOI: 10.1111/j.1600-0889.2006.00202.x

years (Wofsy and Harriss, 2002). However, in order to compare ecosystem-scale information from ground-based observations to atmospherically derived flux patterns, it is necessary to obtain fluxes at a much finer scale than atmospheric inverse methods can currently provide.

The reasons for the inability of inverse studies to yield regional-scale terrestrial carbon fluxes are twofold. First, the CO₂ observational network until a few years ago has concentrated on sampling marine air (Tans et al., 1996; Wofsy and Harriss, 2002), where signals of terrestrial carbon fluxes have been greatly attenuated. Secondly, CO₂ observations in the continental atmosphere exhibit large amplitudes and high-spatiotemporal variability that are difficult for atmospheric models to simulate properly (Gerbig et al., 2003b; Peters et al., 2004). Using error-prone atmospheric models within an inverse study to interpret the large swings in continental CO₂ concentrations can result in highly biased carbon sources/sinks (Gloor et al., 1999).

To address the aforementioned sources of uncertainty, we describe in this paper results from an intensive, aircraft-based atmospheric sampling field programme. The aircraft is uniquely suited to probe distributions both in the vertical and horizontal dimensions and at multiple spatial scales. The specific aircraft sampling programme we focus on—the CO₂ Budget and Rectification Airborne study (COBRA)—is a pilot experiment designed as a first-step to fill in the observational gap. COBRA measured CO₂ profiles within the continental planetary boundary layer (PBL) and up to ~10 km in the free troposphere, and observed the horizontal variability of CO₂ from 10 to 1000 km (Stephens et al., 2000). This data set, resolving the CO₂ in the continental atmosphere at high resolution in both the vertical and the horizontal dimensions, also provides a unique testbed for testing and developing models.

The purpose of this paper is to summarize recent results emerging from COBRA and to suggest the role intensive atmospheric sampling programmes like COBRA can play in helping move forward carbon cycle science. We first provide a description of the COBRA flights that have taken place in 2000, 2003 and 2004 over North America, as well as a brief outline of the on-board sensors (Section 2). Then we illustrate the use of observations from such intensive observations in three different applications: quantifying the spatial variability of CO₂, measuring directly the regional-scale carbon fluxes, and testing atmospheric models (Sections 3–5). We conclude with a look towards the future, outlining ways in which intensive atmospheric sampling can contribute towards advancing carbon science (Section 6).

2. Description of COBRA missions in 2000, 2003 and 2004

2.1. Flight tracks

The COBRA study was conceived as a pilot experiment to conduct intensive atmospheric sampling over the continent. The ob-

jectives were: (a) to observe the horizontal and vertical distribution of CO₂ with sufficient resolution over the continent, formerly lacking in the CO₂ measurement record and (b) to test how to extract information from such highly variable CO₂ observations over the continent (Stephens et al., 2000).

COBRA flights took place during August 2000 in the United States (www-as.harvard.edu/chemistry/cobra/), May–June 2003 over United States and Canada (www.fas.harvard.edu/~cobra/), and May–August 2004 over United States and Canada (www.deas.harvard.edu/cobra/), with particular emphasis on the New England area and Québec. The flight tracks from the three COBRA missions are shown in Fig. 1. These observations are unique in their comprehensive spatial coverage and the intensity of vertical sampling. Such intensive horizontal and vertical sampling cannot be obtained from other means e.g., tower-based CO₂ observations and the weekly to bi-weekly aircraft profiles conducted at a limited number of sites for long-term monitoring (Tans et al., 1996).

All three missions of COBRA carried out both *large-scale surveys* and *regional-scale Lagrangian experiments*. The large-scale surveys were designed to characterize large-scale tracer distributions by having the aircraft conduct profiles every several hundred kilometres between the PBL and the free troposphere. These profiles were often facilitated by the presence of rural airports into which the aircraft can carry out ‘missed approaches’—a flight manoeuvre in which the aircraft descends into an airport but then ascends without actually landing. The regional-scale Lagrangian experiments were envisioned to directly quantify 10–100-km scale carbon fluxes by following CO₂ concentration changes in airmasses as they are advected over the landscape (see Section 4).

Data from a large-scale survey in COBRA-2003 are shown in Fig. 2. This survey consisted of profiles from New Hampshire to Colorado (flight track shown in red in Fig. 2a) conducted between June 27th and 28th. The observations are displayed as altitude versus longitude cross-sections of CO₂ and CO concentrations, constructed from interpolation between the flight locations (marked as grey lines in the cross-sections). Particularly large depletion in CO₂ was observed in the lower troposphere, at ~90°W. Heterogeneity in concentration distributions was observed throughout the atmosphere, even in the free troposphere. In COBRA-2003 the aircraft also conducted numerous profiles into urban plumes to establish tracer signatures in pollution signals, as witnessed by the elevated CO of over 200 ppbv sampled near New York and Baltimore in the eastern part of the cross-section.

Lagrangian experiments took place in 2000 in North Dakota, Wisconsin and Maine. Experiments in Wisconsin and Maine linked the aircraft-derived regional carbon fluxes to concentration and flux measurements on towers: the WLEF tall tower in Wisconsin (Bakwin et al., 1998) and the Howland tower in Maine (Hollinger et al., 1999). COBRA-2003 repeated the Lagrangian experiment near Howland, as well as adding an experiment near

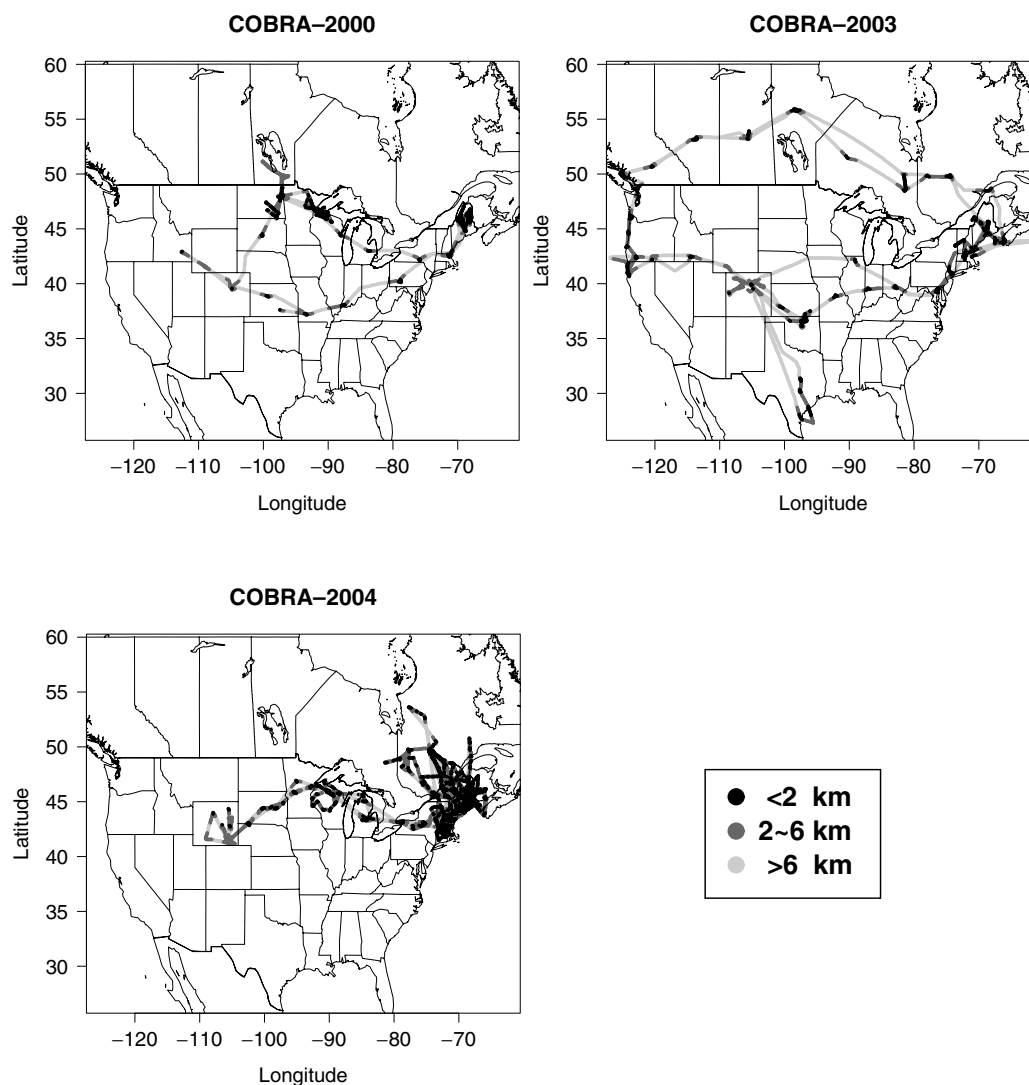


Fig. 1. Flight tracks from the CO₂ Budget and Rectification Airborne (COBRA) study from three different years: August 2000, May–June of 2003, and May–August of 2004. The aircraft altitude above sea-level is shown in grayscale.

the Harvard Forest tower in Massachusetts (Wofsy et al., 1993). In addition, several Lagrangian experiments were carried out near the coasts to examine the transition in CO₂ between continental and marine air. These were conducted over the Gulf of Mexico (Texas), along the Pacific Coast (Oregon), and over the Atlantic, sampling air advected from the northeastern United States to Sable Island, a Canadian long-term observing site (Worthy et al., 2003). COBRA-2004 conducted Lagrangian experiments mainly in the northeastern part of the North American continent, in New England and Québec (Fig. 1). The almost exclusive focus on the northeast was motivated by the following objective: to establish how well regional carbon fluxes in a *limited region* can be constrained, given enhanced atmospheric observational density and extensive biospheric modelling efforts incorporating the atmospheric data and ground-based datastreams

such as eddy covariance, forest inventory analyses and disturbance reconstructions. New England and Québec, with extensive coverage by industrial forests and substantial prior knowledge from forest inventories, was a favourable region for this objective.

2.2. Instrumentation

The aircraft platforms for COBRA were the University of North Dakota Cessna Citation II in 2000 and 2003 and the University of Wyoming King Air in 2004, aircrafts dedicated for scientific research that measure standard meteorological variables such as pressure, temperature, humidity, wind speed and wind direction.

The CO₂ sensor used on-board all the COBRA flights was a modified non-dispersive infrared instrument with in-flight

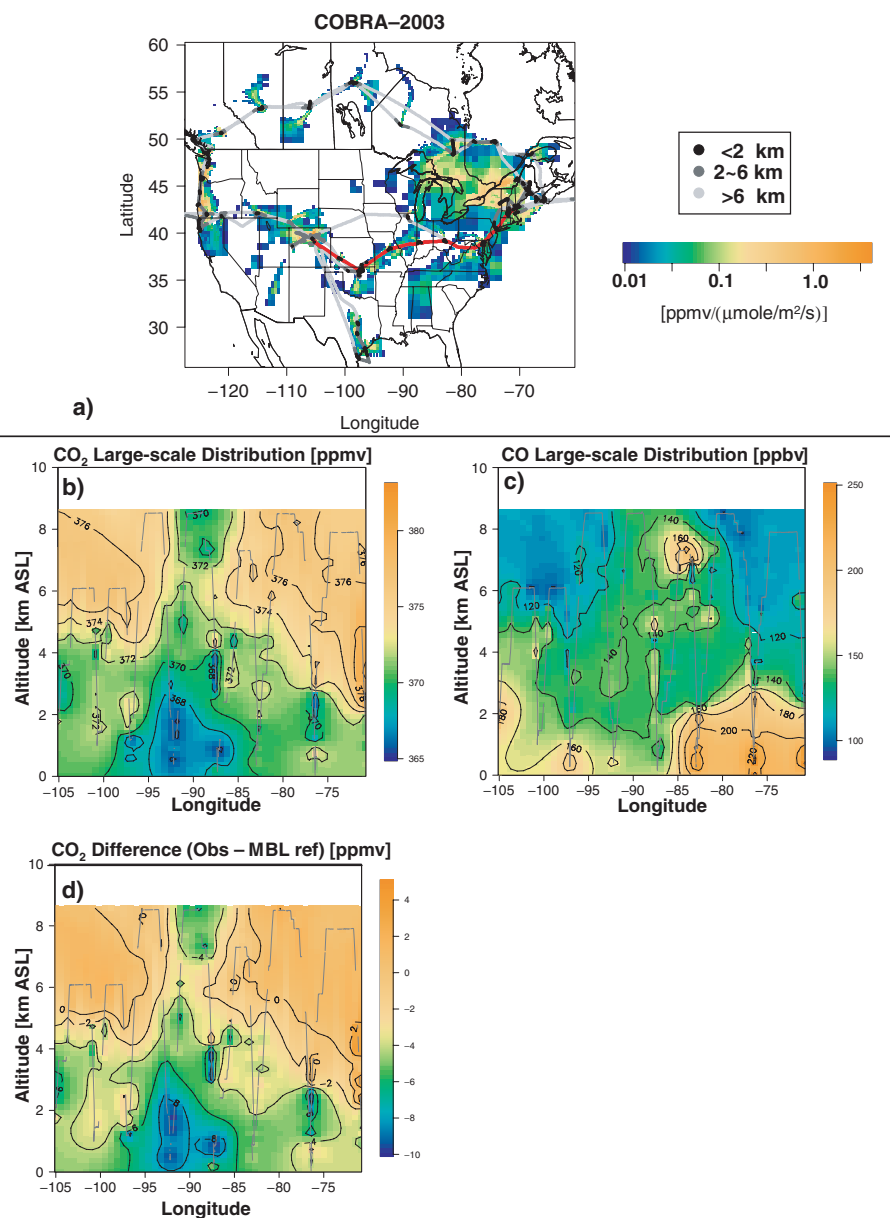


Fig. 2. (a) COBRA-2003 flight tracks and the footprint of observations within the PBL. The footprint was simulated by the STILT atmospheric model (Section 3.3) running backward in time for 3 d. The footprint links atmospheric observations to upstream fluxes, yielding the concentration change (ppmv) for an unit surface flux ($\mu\text{mole}/\text{m}^2/\text{s}$). The footprint is resolved dynamically, at high resolution close to the starting location and is degraded as particles disperse and travel further backward in time. Shown in red is the flight leg used to construct the large-scale tracer cross-sections in (b–d). This survey consisted of profiles from New Hampshire to Colorado conducted between June 27th and 28th 2003. (b and c) Observed altitude versus longitude cross-sections of CO_2 and CO, respectively, derived from interpolation between observations at aircraft locations (grey lines). (d) Differences between observed CO_2 and the marine boundary layer reference value at the same latitude (GLOBALVIEW- CO_2 , 2005; Masarie and Tans, 1995).

calibrations traceable to World Meteorological Organization (WMO) standards to an accuracy of $\pm 0.1\text{ ppmv}$ (Daube et al., 2002). Comparisons with these standards indicated somewhat larger uncertainty of the CO_2 observations of $\pm 0.25\text{ ppmv}$ ($2 - \sigma$) during COBRA-2000 due to a malfunctioning solenoid valve (Daube et al., 2002; Gerbig et al., 2003a).

CO was measured as a combustion tracer to separate out influences of biomass burning and fossil fuel combustion from biospheric activity. CO observations were acquired using a vacuum-UV resonance fluorescence instrument at 1-Hz resolution with a precision of 2 ppbv and a long-term accuracy of 3 ppbv (Gerbig et al., 1999). In 2003, a four-channel gas chromatograph

(Romashkin et al., 2001) was added to the payload, enabling measurement of numerous halocarbon species (Hurst et al., 2006) as well as H₂, CH₄ and N₂O.

3. Application (1): determining spatial variability of CO₂

The high observational density from intensive field sampling programmes like COBRA provides a unique opportunity to probe the spatial variability of CO₂ and to quantify errors resulting from neglecting this variability. We first examine the deviation between free tropospheric CO₂ values and the value observed within the marine boundary layer ('MBL reference'), which has been used as a substitute for free tropospheric values in the absence of direct observations. Then, we focus on the issue of representing a discrete spatial region with a single concentration averaged over a gridcell and disregarding subgridcell variability ('representation errors').

3.1. Marine boundary layer versus free troposphere

The MBL reference CO₂ (Masarie and Tans, 1995) is a latitudinally dependent, weekly varying concentration field constructed from observations within the MBL (GLOBALVIEW-CO₂, 2005). The MBL reference has been used as a surrogate for free tropospheric values over the continent in one-dimensional budgets of regional-scale carbon fluxes from tower-based concentration observations within the continental PBL (Bakwin et al., 2004; Helliker et al., 2004), due to limited observations in the free troposphere and the weaker heterogeneity of free tropospheric CO₂.

The direct observations in the free troposphere from COBRA provided a direct measure of errors resulting from assuming the MBL reference value for the free troposphere. Figure 2d shows the deviation from the MBL reference in the COBRA-2003 large-scale surveys. The large departure of as much as 10 ppmv in the lower troposphere is expected from the proximity to surface fluxes. However, even in the free troposphere departures of 3 ppmv were observed. Enhancements of 3 ppmv above the MBL reference were also reported from COBRA-2000 (Gerbig et al., 2003a).

Such systematic departures of free tropospheric concentrations from the MBL reference over the continent can be explained in large part by advection from different latitudes and by time lags in vertical propagation of concentration changes at the surface—within the MBL—to the free troposphere (Gerbig et al., 2003a).

These systematic deviations of free tropospheric CO₂ from MBL reference values can cause non-negligible biases in the one-dimensional budgets of regional carbon fluxes. These budgets are driven by the CO₂ gradients between the continental PBL and the free troposphere aloft; therefore, errors in free tropospheric CO₂ propagate directly into the calculated carbon flux. Given a

typical vertical CO₂ gradient (PBL-free troposphere) of ~ -10 ppmv during the summer growing season (Bakwin et al., 2004), the carbon sink would be underestimated by 20% just resulting from substituting the MBL reference—which can have a bias error of -2 ppmv during the summer (Fig. 2d)—for the free tropospheric CO₂.

3.2. Representation errors

Spatial variability of a tracer like CO₂ leads to a mismatch between actual observations at a point and the spatial averages observed from space-borne sensors or averages over gridcells simulated by models. This mismatch—the 'representation error'—must be properly quantified and understood. First, this error determines the leverage of point observations to retrieve surface fluxes within an inverse study, which represents concentration fields with gridcell averages.

In other words, the representation error quantifies the degree to which discrepancies between point observations and gridcell averages arise from subgridcell heterogeneity or from signals of differences between assumed versus true fluxes. Thus, neglecting the representation error could overestimate the observational constraint and lead to biased flux solutions (Gerbig et al., 2003b). Secondly, knowledge of the representation error addresses the following question, critical for validation of space-borne sensors: can differences between validation and satellite observations be explained by spatial variability, or does the difference reveal instrument problems (Lin et al., 2004a)?

The large number of vertical profiles conducted within a short period of time during COBRA enabled a first assessment of the spatial variability of CO₂ and the associated representation error. We will not describe here the spatial statistical methodology based on variograms (Kitanidis, 1997) for calculating the spatial variability and the representation error, details of which can be found in Gerbig et al. (2003a).

The representation error as a function of the gridcell size is reproduced from Lin et al. (2004a) and shown in Fig. 3. Discrepancies between column concentrations averaged over different gridcell sizes and the column concentration at a point location are shown for different altitudes in the atmosphere: PBL, 3–6 km and 6–9 km. The representation error is largest for the PBL column, due to the strongly observed spatial heterogeneity in CO₂ within the PBL, in proximity to surface sources/sinks.

The representation error has been shown to be closely related to the error resulting from aggregating upstream surface fluxes (Gerbig et al., 2003b). Degrading upstream fluxes to coarser grids resulted in deviations from fine-scale simulations in simulated CO₂ concentrations that reproduced the representation error curve (Gerbig et al., 2003b). This suggests that the observed representation error is another manifestation of the previously identified 'aggregation error'—the error resulting from aggregating finer-scale fluxes to coarser resolutions (Kaminski et al., 2001). This also means that while gridcell sizes of

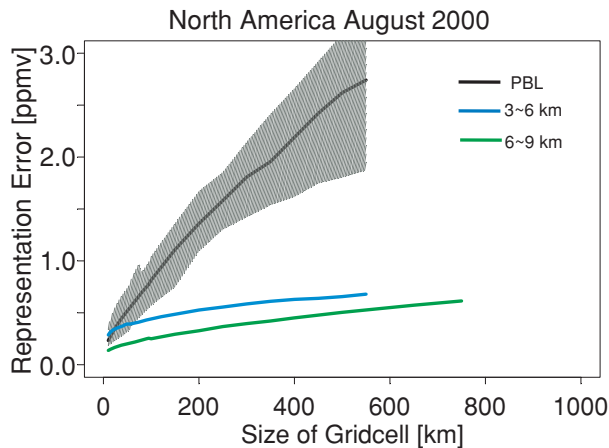


Fig. 3. Representation error—the discrepancy between measurement at a point location and average over a gridcell—as a function of grid cell size, for CO₂ observed during COBRA-2000. The relationship is shown separately for column-averaged CO₂ in the PBL (black), 3–6 km (blue) and 6–9 km (green). The shaded grey region refers to the 95% confidence region for the PBL column.

typical atmospheric models range between 100 and 400 km, the error committed within the PBL could be much larger than the 1–2 ppmv as suggested by Fig. 3, if surface fluxes are actually resolved at scales coarser than the atmospheric gridcells.

Moreover, the representation error may not be random: systematic neglect of subgrid variations in surface fluxes affecting atmospheric concentrations would lead to biased simulations (Gerbig et al., 2003a). For instance, a measurement site with systematic influence from a lake would not show large photosynthetic drawdown in CO₂ concentrations during the growing season (Fig. 4a). A model with gridcells lumping the lake with surrounding forest undergoing photosynthetic uptake would simulate CO₂ concentrations that are systematically lower than observed values, and an inverse analysis using this model that fails to account for the representation/aggregation error would improperly reduce the photosynthetic uptake from the forests.

Just as neglect of subgridscale *spatial* variability leads to errors and biases, neglect of *temporal* variability likewise results in ‘temporal representation errors’ (Lin et al., 2004a). Modelled CO₂ concentrations are often averaged to monthly or even annual values, longer time periods than that characterized by flask data, which sample air over only a few minutes (Conway et al., 1994). Comparisons between simulated monthly averaged and observed instantaneous CO₂ values would differ due to variability within the monthly time window. Future analyses need to quantify this temporal representation error as well as the spatial representation error.

3.3. Modelling framework to resolve variability

The representation error analysis clearly illustrates the need for a modelling framework that can properly interpret the highly

variable continental CO₂ concentrations. Such variability has to be linked to surface fluxes in the near-field of observations at high resolution in order to minimize these aggregation/representation errors and potential biases.

One example of such a modelling framework includes a backward-time transport model that simulates atmospheric transport with Lagrangian particles that represent air parcels. This approach—the Stochastic Time-Inverted Lagrangian Transport (STILT) model (Lin et al., 2003)—links an atmospheric observation to upstream surface fluxes at high spatio-temporal resolution by virtue of its time-reversed formulation. To derive this ‘adjoint’ information (Errico, 1997) at high resolution from a traditional forward-time approach is computationally expensive, necessitating forward-time simulations of unit tracer emissions (e.g., Enting et al. 1995) from all potential gridcells within the source region. Due to this computational cost the conventional forward-time approach has typically limited the number of resolved upstream sources/sinks, resulting in large aggregation/representation errors. In contrast, by tracing air parcels backward in time from the observation location, the upstream source region at different time steps contributing air parcels to the observation location is resolved with a single backward-time simulation, reducing the need for aggregation.

An example of the information derived by STILT is in Fig. 2a, which shows the three day ‘footprint’ for all profiles conducted within the PBL during COBRA-2003, generated by running STILT particles backward in time for 3 days. For these simulations STILT was driven with windfields from the 80-km resolution Eta Data Assimilation System (EDAS). The footprint, in units of [ppmv/($\mu\text{mole}/\text{m}^2/\text{s}$)], provides the linkage between concentrations and surface fluxes and represents the sensitivity of the atmospheric concentration (ppmv) at the starting location to upstream fluxes ($\mu\text{mole}/\text{m}^2/\text{s}$). This sensitivity can be multiplied by modelled carbon fluxes to yield simulated CO₂ concentrations for comparison with observations. The footprint is resolved at higher resolution in the vicinity of the observation to minimize the representation/aggregation error.

Another requirement for the modelling framework follows from the need to account for variability in free tropospheric CO₂ (Fig. 2d), rather than extrapolating from values within the marine boundary layer (Section 3.1). One approach is to construct a boundary condition over the ocean by vertically propagating changes in the marine boundary layer upwards in the atmosphere, and CO₂ values are then advected to the free troposphere over the continent by use of an atmospheric model such as STILT (Gerbig et al., 2003b).

4. Application (2): directly constraining regional-scale fluxes from air-mass-following experiments

The regional-scale Lagrangian experiments conducted during COBRA were designed to yield direct measurements of

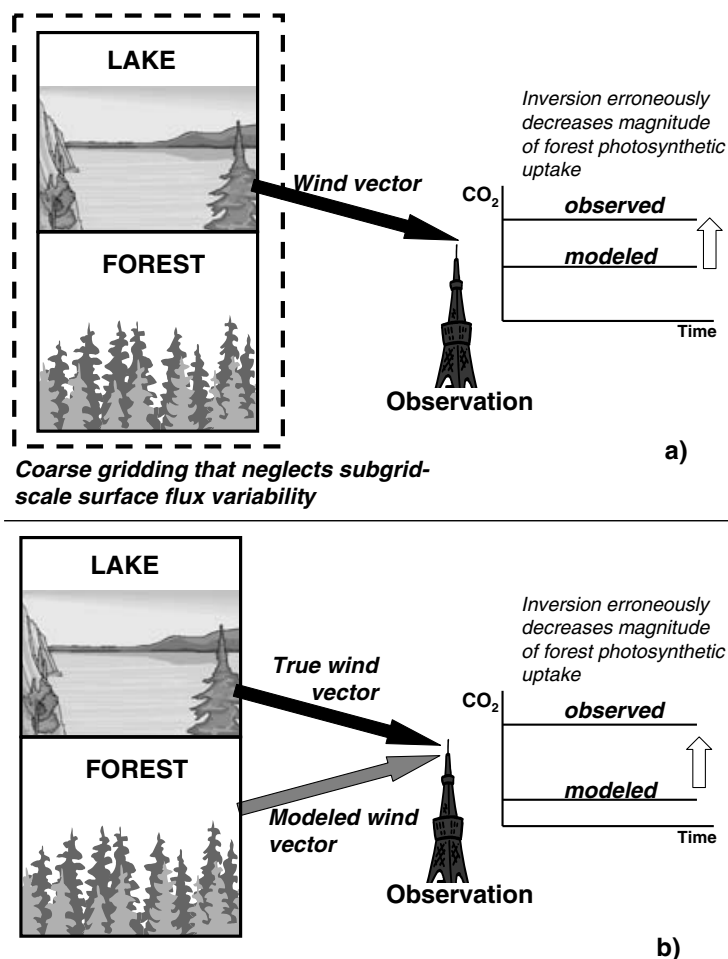


Fig. 4. Schematic diagram illustrating the impact on atmospheric inversions of (a) coarse-scale gridcells that neglect the influence of subgrid-scale fluxes on concentration observations and (b) failure to account for transport errors. These sources of error can cause systematic differences between modelled and observed CO₂ concentrations, resulting in biases in carbon fluxes retrieved from inversions.

regional-scale fluxes in target areas by observing changes in CO₂ concentrations between upwind and downwind locations of airmasses as they move across the landscape. To accomplish this the upwind and downwind sampling locations need to be pre-determined to plan the aircraft flights. During COBRA the STILT model was run operationally with forecasted windfields to predict the airmass locations (Lin et al., 2004b). In COBRA-2004 five forecasted meteorological fields were available to drive STILT, and the model-to-model spread was integrated during flight planning as an indicator of difficulties in predictive capabilities (when different forecasts exhibited significant divergence) or as a way to reduce sensitivity to forecast errors by sampling across the different model predictions.

An example of the observations and results from a single Lagrangian experiment from COBRA-2000 in Maine is shown in Fig. 5. Due to the westerly winds in Maine on this day the morning upstream observations took place to the west of the afternoon, downstream observations in northeastern Maine. The lowest altitudes exhibited marked CO₂ depletion between the upstream and downstream during the day, a signature of regional photosynthetic carbon uptake.

To calculate the regional fluxes the upstream observations were first linked to the downstream observations with the use of the STILT transport model, driven with assimilated windfields (Lin et al., 2004b). Differences (downstream – upstream) in CO₂ column amounts were then divided by the elapsed time to yield the observed fluxes, shown in Fig. 5c. This flux reflects sources/sinks throughout the regional-scale footprint source region (Fig. 5a, right-hand panel).

We stress that such *direct measurement* of the regional-scale carbon flux from airmass-following experiments is unique and difficult to obtain from other means. The airmass-following experiments provide ‘top-down’ constraints at the ~100-km scale (Fig. 5c), much finer than the fluxes provided by previous global inversions. ‘Bottom-up’ measurements like eddy covariance (Wofsy et al., 1993) and inventory studies (Brown and Schroeder, 1999; Barford et al., 2001) measure carbon fluxes with only limited spatial coverage, at local scales (~1 km).

On the other hand, the bottom-up observations can begin to be merged with the finer-scale top-down constraint provided from airmass-following experiments. The observed carbon flux from eddy covariance for the same day at Howland (location shown

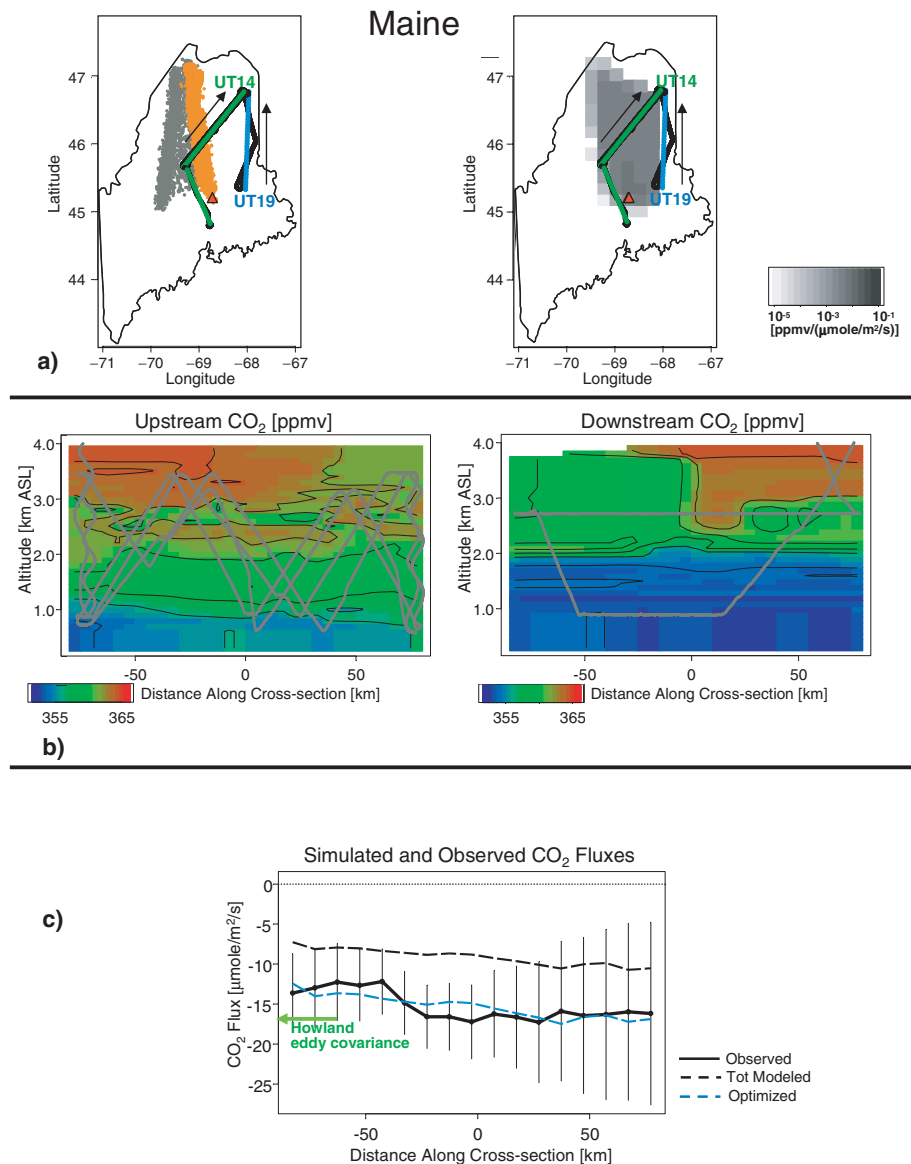


Fig. 5. Lagrangian air mass-following experiment in Maine during COBRA-2000, adapted from Lin et al. (2004b). (a) Left-hand panel: locations of the upstream (green) and downstream (blue) cross-sections sampled during the Lagrangian experiment, as well as the locations of simulated particles (grey and orange) from STILT—started from the downstream cross-section—at the earlier time when the upstream flights were conducted. The particles shown in orange denote those that travelled within the PBL, i.e., particles recently affected by local surface fluxes. The black arrow shows the orientation of the x -axis in the cross-sections shown in (b), pointing in the direction of increasing x . The Howland eddy covariance tower is indicated by the red triangle. (a) Right-hand panel: the footprint of the downstream observations derived from STILT particle locations travelling within the PBL as shown in orange in the left-hand panel. (b) Observed upstream and downstream CO_2 cross-sections from the Lagrangian experiment. Flight paths are shown in grey. The origin refers to the mean horizontal position of the aircraft during the sampling of the cross-section. The x -axis represents the horizontal location along the first principal component of the aircraft locations. (c) The total modelled biospheric CO_2 flux (black dashed), the optimized flux after Bayesian inverse analysis (blue dashed), and the observed biospheric flux derived from the Lagrangian budget (solid black). Negative fluxes denote removal of CO_2 out of the atmosphere, indicative of photosynthetic uptake by the biosphere.

as red triangle in Fig. 5a) is indicated by the green arrow in Fig. 5c. The close correspondence between the regional flux from the atmospheric Lagrangian budget and the local flux derived from eddy covariance in this case reflects the relatively homogeneous coniferous landscape found in northern Maine.

Indeed, merging eddy covariance and other ground-based observations with the air mass-following atmospheric observations is critical for constraining regional-scale (10–1000 km) carbon fluxes over timescales longer than a few days. Directly measured regional carbon fluxes from air mass-following experiments are

restricted to a limited number of days, due to the substantial cost and effort involved in aircraft operations. Eddy covariance fluxes and tower-based concentration observations measure semi-continuously, providing the temporal coverage lacking from the intensive atmospheric measurements.

A preliminary analysis framework that ingests both the eddy covariance and atmospheric observations (from both aircraft intensives and towers) has been constructed (Gerbig et al., 2003b; Lin et al., 2004b). The eddy covariance observations are used to derive parameters within a biospheric model. The regional CO₂ distributions simulated by the biospheric model are then compared against the observed distributions, and differences are used in a Bayesian inversion to optimally adjust the biospheric model. For instance, the simulated CO₂ distribution prior to optimization in the Maine case study yielded magnitudes of carbon uptake (Fig. 5c) less than suggested by the observed CO₂ distribution. Simulated versus observed differences were then minimized in an inversion step that resulted in optimized fluxes (blue dashed line) that are in much closer correspondence with the observed. The optimized fluxes have incorporated information from both the temporally extensive ground-based observations as well as the regionally representative constraint from the atmospheric observations and provides a current best-guess estimate of regional carbon fluxes.

5. Application (3): testing models

The high density of observations from intensive atmospheric sampling is useful not only as input to modelling/analysis frameworks for inferring regional fluxes. These data sets are also crucial for testing and developing such models. Numerous studies have underscored the importance of quantifying and accounting for transport modelling uncertainties in retrieving tracer fluxes from atmospheric observations (Gloor et al., 1999; Peters et al., 2004; Lin and Gerbig, 2005). A simple illustrative example is found in Fig. 4b: given erroneous modelled transport and heterogeneity in upwind sources/sinks, inversion-derived fluxes can be biased.

5.1. Horizontal wind errors

Horizontal tracer variations revealed in the intensive atmospheric observations can be useful for diagnosing errors in horizontal winds, particularly if an independent tracer like CO is available. An example is provided by the Lagrangian air-mass-following experiment conducted in northern Wisconsin, in COBRA-2000 (Fig. 6). The upstream and downstream observations showed large gradients in CO₂ and CO, as well as (not shown) water vapour and temperature. The sharp gradients are likely related to the presence of Lake Superior to the north of the sampling region.

In this example errors in the EDAS windfields used to drive STILT led to significant errors in the retrieved CO₂ and CO

fluxes. The EDAS fields suggested the air found closer to Lake Superior on the right side of the upstream cross-section, with elevated CO₂ and depleted CO, would be advected to the left side of the downstream cross-section, with lowered CO₂ and enhanced CO. This translated into significant CO₂ drawdown and CO release. The inferred CO₂ flux (Fig. 6c) included huge drawdowns of $-40 \mu\text{mole/m}^2/\text{s}$, and the CO flux reached magnitudes characteristic of a non-existent densely populated metropolitan area in northern Wisconsin.

The calculated fluxes in this example were extremely sensitive to errors in horizontal winds due to the sharp gradients in tracer concentrations. In reality, as confirmed by comparison of the EDAS-modelled winds with wind observations onboard the aircraft, the true winds likely advected air from the left side of the upstream—with depleted CO₂ and enhanced CO—to the left side of the downstream—also with lowered CO₂ and elevated CO, thereby lining up the sharp observed horizontal tracer gradient. When wind vectors were corrected the resultant magnitude of CO₂ uptake was lowered and fell into a more reasonable range (Fig. 6d).

The highly heterogeneous distribution of continental CO₂ distributions and fluxes implies that large errors in inferred carbon sources/sinks can result from errors in modelling atmospheric transport, as highlighted by this example. Hence effort must be invested to quantify and incorporate such transport errors into the inversion analysis by, for example, comparison of model-generated windfields to radiosonde observations and including the errors as a stochastic process within the motions of air parcels (Lin and Gerbig, 2005).

5.2. Vertical redistribution errors

In addition to errors in horizontal winds discussed in the previous section, errors in ‘vertical redistribution’ from atmospheric models remain a key uncertainty (Law et al., 1996; Denning et al., 1999; Gurney et al., 2003; Peters et al., 2004). By ‘vertical redistribution’, we refer to atmospheric processes that: (1) determine the vertical extent of the PBL up to which surface fluxes are mixed on hourly timescales (Stull, 1988) and (2) control deep convection which exchanges air between the PBL and the free troposphere (Emanuel, 1994), with significant implications for tracer transport (Thompson et al., 1994).

Uncertainties in vertical redistribution constitute first-order errors that propagate into retrieved fluxes. Put simply, if the atmosphere is considered as on one-dimensional column, the extent of vertical redistribution is the ‘dilution height’ that controls the change in atmospheric concentration resulting from a given surface flux. An alternative perspective is that the modelled footprint for an observation within the PBL (e.g., Fig. 2a) would be decreased (enhanced) if the dilution height is elevated (lowered) or if convection is strengthened (weakened) (Gerbig et al., 2003b).

Errors in vertical redistribution are also closely linked to uncertainties in the ‘rectifier effect’—a key limitation in current

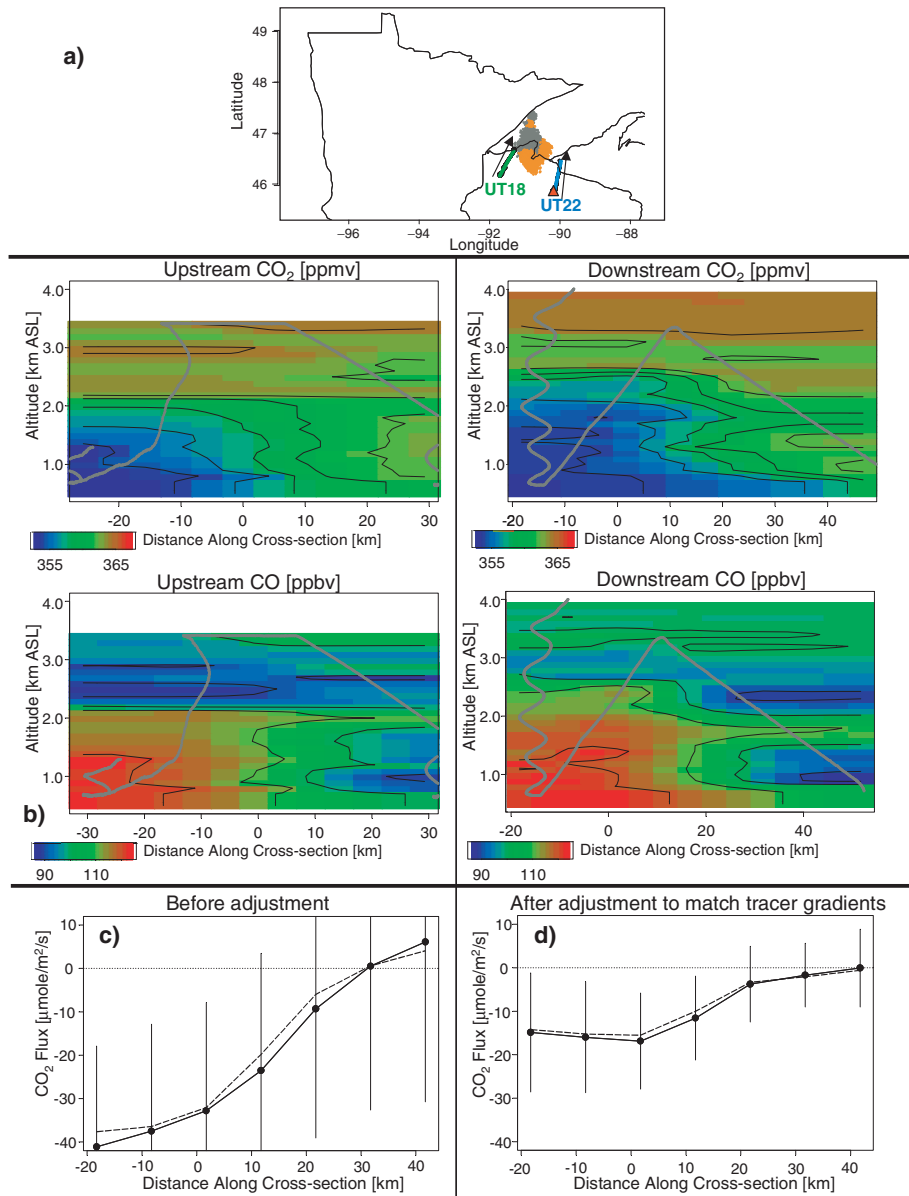


Fig. 6. Lagrangian air mass-following experiment in northern Wisconsin during COBRA-2000, adapted from Lin et al. (2004b). (a) Similar to the left-hand panel in Fig. 5a, with the red triangle denoting location of the WLEF tall tower. (b) Similar to Fig. 5b, but also including CO. (c) Observed biospheric flux derived from the Lagrangian budget, calculated with erroneous modelled winds. The dashed line indicates fluxes prior to correction for combustion emissions (for details see Lin et al. (2004b)). (d) Corrected biospheric flux derived from the Lagrangian budget derived by manual correction of wind vectors by matching observed tracer gradients between the upstream and downstream (see Section 5.1).

inverse analyses (Gurney et al., 2003). The rectifier effect is the temporal covariance between vertical redistribution and the uptake/release of CO_2 that results in a ‘vertical partition of CO_2 ’ (Denning et al., 1999). Differences in the strength of the rectifier effect between global atmospheric transport models have been suggested to lead to critical differences in the carbon sources/sinks derived from inverse analyses (Denning et al., 1999). Similarly, Dargaville et al. (2003) have suggested that how vertical transport partitions CO_2 over the continent is

strongly linked to the interannual variability in interhemispheric CO_2 gradient, which is the signal of interannual variability in the latitudinal gradient in carbon fluxes used by inversions.

The intensive observations from a project like COBRA provide an excellent means for testing vertical redistribution and rectification in atmospheric models. The tracer profiles reveal signatures of vertical mixing that can be used to diagnose model errors. The sharp transitions in tracer concentrations in the lower several km of the atmosphere are indicative of the vertical extent

of mixing in the PBL or the residual ('relic') layer. For instance, the sharp transition in CO₂ concentration in Fig. 5b takes place at ~1 km in the morning upstream observations but increases to an altitude of ~2 km in the afternoon downstream, reflecting the daytime growth of the PBL.

The tracer profiles can also reveal signatures of deep convection. The large-scale vertical profiles from COBRA-2003 show relatively depleted CO₂ of ~370 ppmv and enhanced CO of ~130 ppbv in the free troposphere (4–8 km) at 90°W, in the middle of the United States (Figs. 2b,c). These signatures likely derive from air originally residing in the PBL that has been pumped to higher altitudes from deep convection. Such deep convection signals have proven to be extremely challenging for atmospheric models to reproduce (Law et al., 1996; Gerbig et al., 2003b). Thus, comparisons between intensive tracer observations and modelled distributions are crucial in understanding errors in vertical redistribution and guiding development of methods to simulate convective transport.

6. Summary and conclusions

In this paper, we have summarized intensive CO₂ observations from an aircraft-based atmospheric sampling programme (COBRA) and illustrated their value in characterizing the spatial variability of CO₂, directly constraining regional carbon fluxes, and critically testing models. Another application not mentioned so far is validation of new atmospheric CO₂ column measurements from ground-based Fourier transform spectrometers (Washenfelder et al., 2005) and satellites such as the Orbiting Carbon Observatory (Crisp et al., 2004), which will play increasingly important roles in the future carbon observing system.

Although limited in temporal coverage, intensive atmospheric sampling programmes can play a key role within the context of an integrated research effort such as the North American Carbon Programme (NACP) (Wofsy and Harriss, 2002). As part of the NACP a long-term observational network is being constructed that consists of ground-based CO₂ observations on tall towers and regular aircraft profiles. Intensive atmospheric sampling provides an important complement during targeted periods (e.g., the growing season months) to the long-term observational network, by providing enhanced data sets. The intensive data sets would then be used to: (1) assess the long-term sites' spatial representativity (Section 3); (2) evaluate model performance, for example, simulation of vertical redistribution (Section 5) and (3) directly measure regional fluxes from airmass-following observations (Section 4), which can be used to assess errors in regional fluxes calculated from just the long-term sites.

The intensive CO₂ observations from COBRA have highlighted challenges for models but have also provided a data set for testing and improving models. The significant spatial variability over the continent translates into substantial representation errors that can lead to biased source/sink estimates if the CO₂ concentration fields or fluxes influencing observations are not

properly resolved (Figs. 3 and 4a). The spatial variability would also result in erroneous fluxes in the presence of errors in transport modelling (Figs. 4b and 6c). Conversely, the heterogeneity in continental CO₂ distributions also means that comparisons with simulated distributions serve as a critical test for models. For instance, reproducing the tracer signatures of convective redistribution (Fig. 2b) will serve as a stringent test of atmospheric models and assist in their development.

We have outlined one example of an analysis framework that has the potential to resolve the highly variable CO₂ distributions characterized by COBRA and to relate them to upstream sources/sinks. The framework includes a stochastic time-reversed Lagrangian atmospheric model (STILT) that links point observations to upstream fluxes at high spatiotemporal resolution. The framework further encompasses a biospheric model that incorporates eddy covariance observations and, more recently, new satellite-based biophysical data. Regional fluxes from the biospheric model have been assessed against tall tower-based CO₂ observations and is reported in a separate paper in this Special CO₂ Conference Issue (Matross et al., 2006).

Ultimately, the success of an analysis framework to accurately quantify and project regional carbon fluxes over multiyear or even decadal timescales would depend on more than its ability to resolve the variability in atmospheric CO₂. The framework also needs to: (1) account for model errors (Lin and Gerbig, 2005), with proper consideration of covariances in the errors (Gerbig et al., 2006) and (2) assimilate datastreams characterizing longer-term biospheric processes, such as biomass stock changes from dendrometry or inventory analyses. Multidecadal processes such as forests regrowing from abandoned agricultural fields may be taking up significant amounts of carbon in the eastern United States (Goulden et al., 1996; Brown and Schroeder, 1999). Thus, observations of such long-term biospheric processes need to be combined with the information in atmospheric CO₂ within a single analysis framework in order to understand long-term carbon sources/sinks and inform management practices to increase ecosystem carbon storage.

7. Acknowledgements

We thank the dedicated crew from the University of North Dakota Citation and from the University of Wyoming King Air, with particular appreciation for the skill and professionalism of pilots Paul LeHardy, Tom Drew, and Don Cooksey. COBRA-2000 was jointly funded by the following US agencies: National Science Foundation (ATM-9821044), Department of Energy (DE-FG02-98ER62695), National Aeronautics and Space Administration (NAG5-7950), and National Oceanic and Atmospheric Administration (NA06GP0406). COBRA-2003 was supported by the NASA Large Scale Biosphere-Atmosphere Experiment in Amazonia (NASA NCC5-590). COBRA-2004 was made possible by a grant from the National Science Foundation Biocomplexity in the Environment Programme (ATM-0221850). JCL

was supported by the NASA Earth System Science Fellowship programme and by the NOAA Postdoctoral Programme in Climate and Global Change, administered by the University Corporation for Atmospheric Research.

References

- Bakwin, P. S., Davis, K. J., Yi, C., Wofsy, S. C., Munger, J. W. and co-authors. 2004. Regional carbon dioxide fluxes from mixing ratio data. *Tellus* **56B**, 301–311.
- Bakwin, P. S., Tans, P. P., Hurst, D. F. and Zhao, C. 1998. Measurements of carbon dioxide on very tall towers: results of the NOAA/CMDL program. *Tellus* **50B**, 401–415.
- Barford, C. C., Wofsy, S. C., Goulden, M. L., Munger, J. W., Pyle, E. H. and co-authors. 2001. Factors controlling long- and short-term sequestration of atmospheric CO₂ in a mid-latitude forest. *Science* **294**, 1688–1691.
- Bousquet, P., Ciais, P., Peylin, P., Ramonet, M. and Monfray, P. 1999. Inverse modeling of annual atmospheric CO₂ sources and sinks 1. method and control inversion. *J. Geophys. Res.* **104**(D21), 26161–26178.
- Brown, S. L. and Schroeder, P. E. 1999. Spatial patterns of aboveground production and mortality of woody biomass for eastern U.S. forests. *Ecol. Appl.* **9**(3), 968–980.
- Conway, T. J., Tans, P. P., Waterman, L. S., Thoning, K. W., Kitzis, D. R. and co-authors. 1994. Evidence for interannual variability of the carbon cycle from the National Oceanic and Atmospheric Administration/Climate Monitoring and Diagnostics Laboratory Global Air Sampling Network. *J. Geophys. Res.* **99**(D11), 22831–22855.
- Crisp, D., Atlas, R. M., Breon, F.-M., Brown, L. R., Burrows, J. P. and co-authors. 2004. The Orbiting Carbon Observatory (OCO) mission. *Adv. Space Res.* **34**, 700–709.
- Dargaville, R. J., Doney, S. C. and Fung, I. Y. 2003. Inter-annual variability in the interhemispheric atmospheric CO₂ gradient: contributions from transport and the seasonal rectifier. *Tellus* **55B**, 711–722.
- Daube, B. C., Boering, K. A., Andrews, A. E. and Wofsy, S. C. 2002. A high-precision fast-response airborne CO₂ analyzer for in situ sampling from the surface to the middle stratosphere. *J. Atmos. Ocean. Technol.* **19**, 1532–1543.
- Denning, A. S., Takahashi, T. and Friedlingstein, P. 1999. Can a strong atmospheric CO₂ rectifier effect be reconciled with a “reasonable” carbon budget? *Tellus* **51B**, 249–253.
- Emanuel, K. A. 1994. *Atmospheric Convection*. Oxford University Press.
- Enting, I. G., Trudinger, C. M. and Francey, R. J. 1995. A synthesis inversion of the concentration and delta-C-13 of atmospheric CO₂. *Tellus* **47B**(1–2), 35–52.
- Errico, R. M. 1997. What is an adjoint model? *Bull. Am. Meteor. Soc.* **78**(11), 2577–2591.
- Fan, S., Gloor, M., Mahlman, J., Pacala, S., Sarmiento, J. and co-authors. 1998. A large terrestrial carbon sink in North America implied by atmospheric and oceanic carbon dioxide data and models. *Science* **282**, 442–446.
- Gerbig, C., Schmitgen, S., Kley, D., Volz-Thomas, A., Dewey, K. and co-authors. 1999. An improved fast-response vacuum-UV resonance fluorescence CO instrument. *J. Geophys. Res.* **104**(D1), 1699–1704.
- Gerbig, C., Lin, J. C., Wofsy, S. C., Daube, B. C., Andrews, A. E. and co-authors. 2003a. Toward constraining regional-scale fluxes of CO₂ with atmospheric observations over a continent: 1. observed spatial variability from airborne platforms. *J. Geophys. Res.* **108**(D24), 4756, doi:10.1029/2002JD003018.
- Gerbig, C., Lin, J. C., Wofsy, S. C., Daube, B. C., Andrews, A. E. and co-authors. 2003b. Toward constraining regional-scale fluxes of CO₂ with atmospheric observations over a continent: 2. analysis of COBRA data using a receptor-oriented framework. *J. Geophys. Res.* **108**(D24), 4757, doi:10.1029/2003JD003770.
- Gerbig, C., Lin, J. C., Munger, J. W. and Wofsy, S. C. 2006. What can tracer observations in the continental boundary layer tell us about surface-atmosphere fluxes? *Atmos. Chem. Phys.* **6**, 539–554.
- GLOBALVIEW-CO₂, 2005. GLOBALVIEW-CO₂: Cooperative atmospheric data integration project—carbon dioxide. National Oceanic and Atmospheric Administration/Climate Monitoring and Diagnostics Laboratory, Boulder, Colorado.
- Gloor, M., Fan, S.-M., Pacala, S., Sarmiento, J. and Ramonet, M. 1999. A model-based evaluation of inversions of atmospheric transport, using annual mean mixing ratios, as a tool to monitor fluxes of nonreactive trace substances like CO₂ on a continental scale. *J. Geophys. Res.* **104**(D12), 14 245–14 260.
- Goulden, M. L., Munger, J. W., Fan, S.-M., Daube, B. C. and Wofsy, S. C. 1996. Exchange of carbon dioxide by a deciduous forest: response to interannual climate variability. *Science* **271**, 1576–1578.
- Gurney, K. R., Law, R. M., Denning, A. S., Rayner, P. J., Baker, D. and co-authors. 2002. Towards robust regional estimates of CO₂ sources and sinks using atmospheric transport models. *Nature* **415**, 626–630.
- Gurney, K. R., Law, R. M., Denning, A. S., Rayner, P. J., Baker, D. and co-authors. 2003. TransCom 3 CO₂ inversion intercomparison: 1 annual mean control results and sensitivity to transport and prior flux information. *Tellus* **55B**, 555–579.
- Helliker, B. R., Berry, J. A., Betts, A. K., Bakwin, P. S., Davis, K. J. and co-authors. 2004. Estimates of net CO₂ flux by application of equilibrium boundary layer concepts to CO₂ and water vapor measurements from a tall tower. *J. Geophys. Res.* **109**(D20106), doi:10.1029/2004JD004532.
- Hollinger, D. Y., Goltz, S. M., Davidson, E. A., Lee, J. T., Tu, K. and co-authors. 1999. Seasonal patterns and environmental control of carbon dioxide and water vapor exchange in an ecotonal boreal forest. *Global Change Biol.* **5**, 891–902.
- Hurst, D., Lin, J. C., Romashkin, P. A., Daube, B. C., Gerbig, C. and co-authors. 2006. Continuing emissions of restricted halocarbons in the USA and Canada: Are they still globally significant? *J. Geophys. Res.* **111**(D15302), doi:10.1029/2005JD006785.
- Kaminski, T., Rayner, P. J., Heimann, M. and Enting, I. G. 2001. On aggregation errors in atmospheric transport inversions. *J. Geophys. Res.* **106**(D5), 4703–4715.
- Keeling, C. D., Bacastow, R. B., Bain-Bridge, A. E., Ekdahl, C. A., Jr., Guenther, P. R. and co-authors. 1976. Atmospheric carbon dioxide variations at Mauna Loa Observatory, Hawaii. *Tellus* **28**, 538–551.
- Kitanidis, P. K. 1997. *Introduction to Geostatistics: Applications in Hydrogeology*. Cambridge University Press, Cambridge, UK, 271 pp.
- Law, R. M., Rayner, P. J., Denning, A. S., Erickson, D., Fung, I. Y. and co-authors. 1996. Variations in modeled atmospheric transport of carbon dioxide and the consequences for CO₂ inversions. *Global Biogeochem. Cycles* **10**(4), 783–796.

- Lin, J. C. and Gerbig, C. 2005. Accounting for the effect of transport errors on tracer inversions. *Geophys. Res. Lett.* **32**(L01802), doi:10.1029/2004GL021127.
- Lin, J. C., Gerbig, C., Wofsy, S. C., Andrews, A. E., Daube, B. C. and co-authors. 2003. A near-field tool for simulating the upstream influence of atmospheric observations: the Stochastic Time-Inverted Lagrangian Transport (STILT) model. *J. Geophys. Res.* **108**(D16), 4493, doi:10.1029/2002JD003161.
- Lin, J. C., Gerbig, C., Wofsy, S. C., Andrews, A. E., Vay, S. A. and co-authors. 2004a. An empirical analysis of the spatial variability of atmospheric CO₂: implications for inverse analyses and space-borne sensors. *Geophys. Res. Lett.* **31**(L23104), doi:10.1029/2004GL020957.
- Lin, J. C., Gerbig, C., Wofsy, S. C., Andrews, A. E., Daube, B. C. and co-authors. 2004b. Measuring fluxes of trace gases at regional scales by Lagrangian observations: application to the CO₂ Budget and Rectification Airborne (COBRA) study. *J. Geophys. Res.* **109**(D15304), doi:10.1029/2004JD004754.
- Masarie, K. A. and Tans, P. P. 1995. Extension and integration of atmospheric carbon dioxide data into a globally consistent measurement record. *J. Geophys. Res.* **100**, 11 593–11 610.
- Matross, D. M., Andrews, A. E., Pathmathevan, M., Gerbig, C., Lin, J. C. and co-authors. 2007. Estimating regional carbon exchange in New England and Quebec by combining atmospheric, ground-based, and satellite data. *Tellus-B*, this issue.
- Peters, W., Krol, M. C., Dlugokencky, E. J., Dentener, F. J., Bergamaschi, P. and co-authors. 2004. Toward regional-scale modeling using the two-way nested global model TM5: characterization of transport using SF₆. *J. Geophys. Res.* **109**(D19314), doi:10.1029/2004JD005020.
- Romashkin, P. A., Hurst, D. F., Elkins, J. W., Dutton, G. S., Fahey, D. W. and co-authors. 2001. In situ measurements of long-lived trace gases in the lower stratosphere by gas chromatography. *J. Atmos. Ocean. Technol.* **18**, 1195–1204.
- Schimmel, D., Melillo, J., Tian, H., McGuire, A. D., Kicklighter, D. and co-authors. 2000. Contribution of increasing CO₂ and climate to carbon storage by ecosystems in the United States. *Science* **287**, 2004–2006.
- Stephens, B. B., Wofsy, S. C., Keeling, R. F., Tans, P. P., and Potosnak, M. J. 2000. The CO₂ budget and rectification airborne study: strategies for measuring rectifiers and regional fluxes. In: *Inverse Methods in Global Biogeochemical Cycles* (eds. Kasibhatla P., et al.). American Geophysical Union, Washington, DC, pp. 311–324.
- Stull, R. B. 1988. *An Introduction to Boundary Layer Meteorology*. Kluwer, Dordrecht, The Netherlands, 666 pp.
- Tans, P. P., Bakwin, P. S. and Guenther, D. W. 1996. A feasible Global Cycle Observing System: a plan to decipher today's carbon cycle based on observations. *Global Change Biol.* **2**, 309–318.
- Tans, P. P., Fung, I. Y. and Takahashi, T. 1990. Observational constraints on the global atmospheric CO₂ budget. *Science* **247**, 1431–1438.
- Thompson, A. M., Pickering, K. E., Dickerson, R. R., Ellis, W. G., Jr., Jacob, D. J. and co-authors. 1994. Convective-transport over the central United States and its role in regional CO and ozone budgets. *J. Geophys. Res.* **99**(D9), 18 703–18 711.
- Washenfelder, R. A., Sherlock, V., Connor, B. J., Toon, G. C. and Wennberg, P. O. 2005. Initial results from the total carbon column observing network. 7th International Carbon Dioxide Conference, Broomfield, CO.
- Wofsy, S. C. and Harriss, R. C. 2002. The North American Carbon Program (NACP), NACP Committee of the U.S. Interagency Carbon Cycle Science Program, U.S. Global Change Research Program, Washington, DC.
- Wofsy, S. C., Goulden, M. L., Munger, J. W., Fan, S.-M., Bakwin, P. S. and co-authors. 1993. Net exchange of CO₂ in a mid-latitude forest. *Science* **260**, 1314–1317.
- Worthy, D. E. J., Higuchi, K. and Chan, D. 2003. North American influence on atmospheric carbon dioxide data collected at Sable Island, Canada. *Tellus* **55B**, 105–114.